

Observations from the 8-Tetrahedron Nonorientable Census

Benjamin A. Burton

CONTENTS

- 1. Introduction
 - 2. Constructing Minimal Triangulations
 - 3. Observations and Conjectures
 - 4. Appendix: Triangulations from the Census
- Acknowledgments
References

Through computer enumeration with the aid of topological results, we catalogue all 18 closed nonorientable \mathbb{P}^2 -irreducible 3-manifolds that can be formed from eight or fewer tetrahedra. In addition, we give an overview as to how the 100 resulting minimal triangulations are constructed. Observations and conjectures are drawn from the census data, and future potential for the nonorientable census is discussed. Some preliminary 9-tetrahedron results are also included.

1. INTRODUCTION

Several surveys have been performed in recent years of all small 3-manifold triangulations satisfying particular properties. One of the key strengths of such a census is in examining *minimal triangulations* (triangulations of 3-manifolds that use as few tetrahedra as possible).

Minimal triangulations are still poorly understood. Many necessary conditions for minimality can be found in the literature; see [Matveev 98], [Martelli and Petronio 01], [Jaco and Rubinstein 03], and [Burton 04a] for some examples. However, sufficient conditions are much more difficult to find. Most of the positive results regarding minimality rely on exhaustive censuses such as these.

Beyond its use in studying minimal triangulations, a census also forms a useful body of examples for testing conjectures and searching for patterns. Section 3 illustrates some conjectures arising from the nonorientable census described in this paper.

We restrict our attention here to closed \mathbb{P}^2 -irreducible 3-manifolds. Examples of other censuses involving manifolds with boundaries or cusps can be seen in the results of Callahan, Hildebrand, and Weeks [Callahan et al. 99] and Frigerio, Martelli, and Petronio [Frigerio et al. 03].

The extent of census data known to date for minimal 3-manifold triangulations is fairly small. This is due to the computational difficulty of performing such

2000 AMS Subject Classification: Primary 57Q15;
Secondary 57-04, 57N10

Keywords: Minimal triangulation, census, complexity, layering

a survey—the number of potential triangulations to examine grows worse than exponentially with the number of tetrahedra.

Closed orientable 3-manifolds have been surveyed successively by Matveev for six tetrahedra [Matveev 98], Ovchinnikov for seven tetrahedra, Martelli and Petronio for nine tetrahedra [Martelli and Petronio 01], and more recently Martelli for ten tetrahedra [Martelli 06] and Matveev for eleven tetrahedra [Matveev 05].

Closed nonorientable 3-manifolds are less-well studied. The 6-tetrahedron and 7-tetrahedron cases were tackled independently by Amendola and Martelli and by Burton [Amendola and Martelli 03, Amendola and Martelli 05, Burton 03]. Only eight different nonorientable 3-manifolds are found up to seven tetrahedra, and none at all are found below six tetrahedra. In this sense, the 7-tetrahedron results are but a taste of what lies ahead.

The methods of these different authors are notably distinct. Amendola and Martelli do not use a direct computer search, but instead employ more-creative techniques. For seven tetrahedra [Amendola and Martelli 05] they examine orientable double covers and invoke the results of the 9-tetrahedron orientable census [Martelli and Petronio 01]. More remarkable is their 6-tetrahedron census [Amendola and Martelli 03], which is purely theoretical and makes no use of computers at all.

On the other hand, Burton focuses on minimal triangulations of these eight different 3-manifolds and their combinatorial structures. With three exceptions in the smallest case (six tetrahedra), the compositions of the 41 different minimal triangulations found in the census are described in detail and generalized into infinite families [Burton 03].

It is also worth noting the work of Casali, who has used the theory of crystallizations to build a catalogue of nonorientable colored triangulations [Casali 98]. This catalogue has since been used to replicate and improve upon the earlier results of Amendola and Martelli [Casali 04].

The work presented here extends the nonorientable-census results to eight tetrahedra. Both 3-manifolds and all their minimal triangulations are enumerated and placed in the context of earlier results. In total, there are 10 new 3-manifolds with 59 different triangulations. All 59 of these minimal triangulations fit within the families described in [Burton 03].

It is worth noting that the list of nonorientable 3-manifolds formed from eight or fewer tetrahedra is equivalently a list of nonorientable 3-manifolds with Matveev complexity less than or equal to 8. Matveev defines the

complexity of a 3-manifold in terms of special spines [Matveev 90], and it is proven in [Martelli and Petronio 02] that for all closed \mathbb{P}^2 -irreducible 3-manifolds other than S^3 , $\mathbb{R}P^3$, and $L_{3,1}$, this is equivalent to the number of tetrahedra in a minimal triangulation (in the orientable case this was proven by Matveev over a decade earlier [Matveev 90]).

All of the computational work was performed using *Regina*, a software package that performs a variety of different calculations and procedures in 3-manifold topology [Burton 04b, Burton 05].¹

In the remainder of Section 1 we describe in detail the census parameters and give a concise summary of the results. Section 2 presents an overview of how the different minimal triangulations are constructed, though the reader is referred to [Burton 03] for finer details (an appendix is provided to match the individual census triangulations to the detailed constructions of [Burton 03]). Finally, Section 3 contains some observations and conjectures drawn from the census results, and closes with some remarks regarding future directions of the nonorientable census. Partial results from the 9-tetrahedron census (which is currently under construction) are briefly discussed.

1.1 Summary of Results

As with the previous closed censuses described above, we consider only triangulations satisfying the following constraints:

- *Closed*: The triangulation is of a closed 3-manifold. In particular, it has no boundary faces, and each vertex link is a 2-sphere.
- \mathbb{P}^2 -*irreducible*: The underlying 3-manifold has no embedded two-sided projective planes, and furthermore every embedded 2-sphere bounds a ball.
- *Minimal*: The underlying 3-manifold cannot be triangulated using fewer tetrahedra.

Tetrahedra	3-Manifolds	Triangulations
≤ 5	0	0
6	5	24
7	3	17
8	10	59
Total:	18	100

TABLE 1. Summary of closed nonorientable census results.

¹The program *Regina*, its source code, and accompanying documentation are freely available from <http://regina.sourceforge.net/>.

Tetrahedra	3-Manifold	Triangulations	Homology
6	$T^2 \times I / \begin{bmatrix} 1 & 1 \\ 1 & 0 \end{bmatrix}$	1	\mathbb{Z}
	$T^2 \times I / \begin{bmatrix} 0 & 1 \\ 1 & 0 \end{bmatrix}$	6	$\mathbb{Z} \oplus \mathbb{Z}$
	$T^2 \times I / \begin{bmatrix} 1 & 0 \\ 0 & -1 \end{bmatrix}$	3	$\mathbb{Z} \oplus \mathbb{Z} \oplus \mathbb{Z}_2$
	SFS $(\mathbb{R}P^2 : (2, 1) (2, 1))$	9	$\mathbb{Z} \oplus \mathbb{Z}_4$
	SFS $(\bar{D} : (2, 1) (2, 1))$	5	$\mathbb{Z} \oplus \mathbb{Z}_2 \oplus \mathbb{Z}_2$
7	$T^2 \times I / \begin{bmatrix} 2 & 1 \\ 1 & 0 \end{bmatrix}$	4	$\mathbb{Z} \oplus \mathbb{Z}_2$
	SFS $(\mathbb{R}P^2 : (2, 1) (3, 1))$	10	\mathbb{Z}
	SFS $(\bar{D} : (2, 1) (3, 1))$	3	$\mathbb{Z} \oplus \mathbb{Z}_2$
8	$T^2 \times I / \begin{bmatrix} 3 & 1 \\ 1 & 0 \end{bmatrix}$	10	$\mathbb{Z} \oplus \mathbb{Z}_3$
	$T^2 \times I / \begin{bmatrix} 3 & 2 \\ 2 & 1 \end{bmatrix}$	2	$\mathbb{Z} \oplus \mathbb{Z}_2 \oplus \mathbb{Z}_2$
	SFS $(\mathbb{R}P^2 : (2, 1) (4, 1))$	10	$\mathbb{Z} \oplus \mathbb{Z}_2$
	SFS $(\mathbb{R}P^2 : (2, 1) (5, 2))$	10	\mathbb{Z}
	SFS $(\mathbb{R}P^2 : (3, 1) (3, 1))$	7	$\mathbb{Z} \oplus \mathbb{Z}_6$
	SFS $(\mathbb{R}P^2 : (3, 1) (3, 2))$	9	$\mathbb{Z} \oplus \mathbb{Z}_3$
	SFS $(\bar{D} : (2, 1) (4, 1))$	3	$\mathbb{Z} \oplus \mathbb{Z}_2 \oplus \mathbb{Z}_2$
	SFS $(\bar{D} : (2, 1) (5, 2))$	3	$\mathbb{Z} \oplus \mathbb{Z}_2$
	SFS $(\bar{D} : (3, 1) (3, 1))$	3	$\mathbb{Z} \oplus \mathbb{Z}_3$
SFS $(\bar{D} : (3, 1) (3, 2))$	2	$\mathbb{Z} \oplus \mathbb{Z}_3$	

TABLE 2. Details for each closed nonorientable \mathbb{P}^2 -irreducible 3-manifold.

Requiring triangulations to be \mathbb{P}^2 -irreducible and minimal keeps the number of triangulations down to manageable levels, focusing only on the simplest triangulations of the simplest 3-manifolds (from which more-complex 3-manifolds can be constructed).

The main result of this paper is Theorem 1.1 below. As with most censuses described in the literature, its proof relies on an exhaustive computer search. This search was performed using the software package *Regina*, with the help of several results described in [Burton 04a] to increase the efficiency of the search algorithm. For an overview of how the search algorithm is structured, see the 7-tetrahedron census paper [Burton 03].

Theorem 1.1. (Census results.) *Consider all closed nonorientable \mathbb{P}^2 -irreducible 3-manifolds that can be triangulated using at most eight tetrahedra. This set contains 18 different 3-manifolds with a total of 100 minimal triangulations between them, as summarized in Tables 1 and 2.*

It should be noted that, when restricted to at most seven tetrahedra, the eight different 3-manifolds obtained match precisely the lists presented in [Amendola and Martelli 05].

For complete details of the 100 minimal triangulations, a data file may be downloaded from the *Regina* web site [Burton 05].² When opened within *Regina*, the triangulations may be examined in detail along with various properties of interest such as algebraic invariants and normal surfaces.

As promised in Theorem 1.1, a brief summary of results appears in Table 1. Here we see overall totals, split according to the number of tetrahedra in the minimal triangulations for each 3-manifold. Note that each triangulation is counted once up to isomorphism, i.e., a relabeling of the tetrahedra within the triangulation and their individual faces.

²The 8-tetrahedron nonorientable census data are also bundled with *Regina* version 4.2.1 or later. They can be found in the *File* → *Open Example* menu.

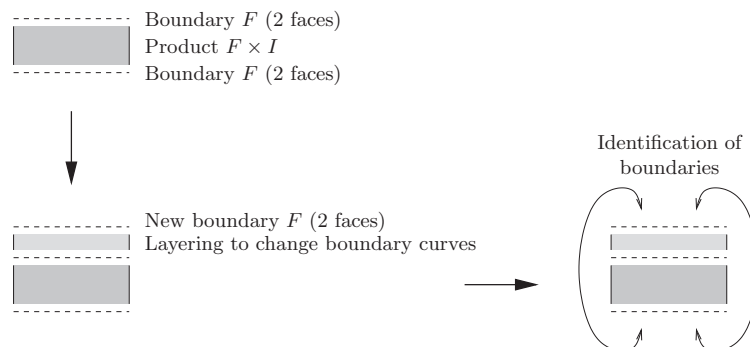


FIGURE 1. Constructing a layered surface bundle.

Two striking observations can be made from Table 1, which have been made before [Amendola and Martelli 05, Burton 03] but are worth repeating here. These are that (i) there are no closed nonorientable \mathbb{P}^2 -irreducible triangulations at all with five or fewer tetrahedra, and that (ii) the number of minimal triangulations is much larger than the number of 3-manifolds. Indeed, most 3-manifolds in the census can be realized by several different minimal triangulations, as seen again in the next table.

Table 2 provides finer detail for each of the 18 different 3-manifolds, including the number of minimal triangulations for each 3-manifold and the first homology group. The notation used for describing 3-manifolds is as follows:

- $T^2 \times I / \begin{bmatrix} p & q \\ r & s \end{bmatrix}$ represents the torus bundle over the circle with monodromy $\begin{bmatrix} p & q \\ r & s \end{bmatrix}$;
- $SFS(B : \dots)$ represents a nonorientable Seifert fibered space over the base orbifold B , where $\mathbb{R}P^2$ and \bar{D} represent respectively the projective plane and the disk with reflector boundary. The remaining arguments (...) describe the exceptional fibers.

The most immediate observation is that the 8-tetrahedron census offers little more variety than the 6- and 7-tetrahedron censuses that came before it. The census is populated entirely by torus bundles and by Seifert fibered spaces over $\mathbb{R}P^2$ or \bar{D} with two exceptional fibers. Preliminary results suggest that the 9-tetrahedron census will reveal more variety than this; see Section 3 for further discussion.

Finally, it is worth noting that, as observed by Amendola and Martelli [Amendola and Martelli 03], all four flat Klein-bottle bundles can be triangulated with only six tetrahedra. These include all 6-tetrahedron manifolds in the table except for $T^2 \times I / \begin{bmatrix} 1 & 1 \\ 1 & 0 \end{bmatrix}$.

2. CONSTRUCTING MINIMAL TRIANGULATIONS

In the 7-tetrahedron census paper [Burton 03], the combinatorial structures of the 41 census triangulations are described in full detail. A number of parameterized families are presented, precise parameterized constructions are given for triangulations in these families, and the resulting 3-manifolds are identified.

The census having been extended to eight tetrahedra, all of the additional 59 triangulations are found to belong to these same parameterized families. We therefore refer the reader to [Burton 03] for details of their construction. Here we present a simple overview of each family, showing how their triangulations are pieced together to form 3-manifolds of various types. We go into some detail, since these families feature in some of the conjectures of Section 3.

For completeness, the appendix (Section 4) contains a full listing with the precise parameters for each census triangulation. This allows the triangulations to be fully reconstructed and cross-referenced against [Burton 03], though of course the reader is invited to download the 100 triangulations instead as a *Regina* data file as described in the introduction.

There are three broad families of triangulations to describe. These are the layered surface bundles, the plugged thin I -bundles, and the plugged thick I -bundles. Each is discussed in its own section below.

2.1 Layered Surface Bundles

A *layered surface bundle* is a triangulation that produces either a torus bundle or a Klein-bottle bundle over the circle.³ We postpone a formal definition for the moment, instead giving a broad overview of the construction.

³The name “layered surface bundle” has been chosen for consistency with related families of triangulations such as layered solid tori and layered lens spaces, as described in [Jaco and Rubinstein 03] and elsewhere.

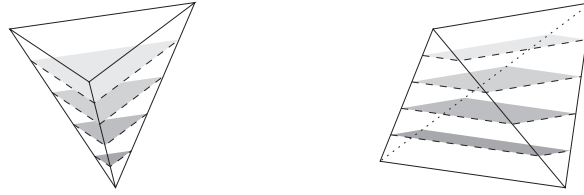


FIGURE 2. Decomposing a tetrahedron into triangles or quadrilaterals.

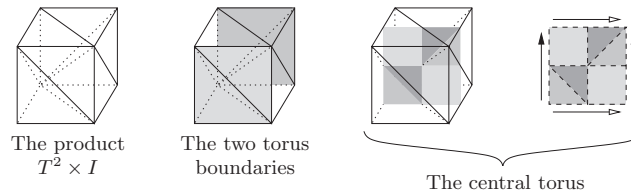


FIGURE 3. An example of a thin I -bundle over the torus.

Figure 1 illustrates the general structure of a layered surface bundle. Note that this is a rough outline only; much of Section 2.1.1 is devoted to filling in the details. First, the product $T^2 \times I$ or $K^2 \times I$ is constructed (where the surface F in the diagram is either T^2 or K^2 for the torus or Klein bottle accordingly). This leaves two boundary surfaces, which are then identified according to some specified monodromy. If this is impossible because the boundary edges do not match, some additional tetrahedra may be layered onto one of the boundary surfaces to adjust the boundary edges accordingly.

2.1.1 Components. We continue with enough detail to allow a precise definition of a layered surface bundle as seen in Definition 2.3 below. This requires us to describe more precisely how the product $T^2 \times I$ or $K^2 \times I$ is formed, as well as what a layering entails.

Definition 2.1. (Untwisted thin I -bundle.) An *untwisted thin I -bundle* over some closed surface F is a triangulation of the product $F \times I$ formed as follows.

Consider the interval $I = [0, 1]$. The product $F \times I$ is naturally foliated by surfaces $F \times \{x\}$ for $x \in [0, 1]$. When restricted to an individual tetrahedron, we require that this foliation decompose the tetrahedron into either triangles or quadrilaterals as illustrated in Figure 2. We furthermore require that every vertex lie on one of the boundaries $F \times \{0\}$, $F \times \{1\}$, as do the upper face in the triangular case and the upper and lower edges in the quadrilateral case.

In particular, the surface $F \times \{\frac{1}{2}\}$ meets every tetrahedron in precisely one triangle or quadrilateral. We refer to $F \times \{\frac{1}{2}\}$ as the *central surface* of the I -bundle.

An example of an untwisted thin I -bundle over the torus is illustrated in Figure 3. This triangulation consists of six tetrahedra arranged into a cube. The front and back faces of the cube form the boundary tori, which are shaded in the second diagram of the sequence. The remaining faces are identified in the usual way for a torus (the top identified with the bottom and the left identified with the right).

The central surface $T^2 \times \{\frac{1}{2}\}$ is shown in the third diagram. In the fourth diagram we can see precisely how the six tetrahedra divide this central torus into six cells, each a triangle or quadrilateral, with the arrows indicating which edges are identified with which.

It follows from Definition 2.1 that a thin I -bundle is “only one tetrahedron thick.” That is, each tetrahedron runs all the way from one boundary surface to the other, as does each nonboundary edge.

As a final note, it should be observed that the decomposition of the central surface offers enough information to completely reconstruct the thin I -bundle. This is because each triangle or quadrilateral of the central surface corresponds to one tetrahedron, and the adjacencies of the triangles and quadrilaterals dictate the corresponding adjacencies between tetrahedra.

We move now to describe a layering, a well-known procedure by which a single tetrahedron is attached to a boundary surface in order to rearrange the boundary edges.

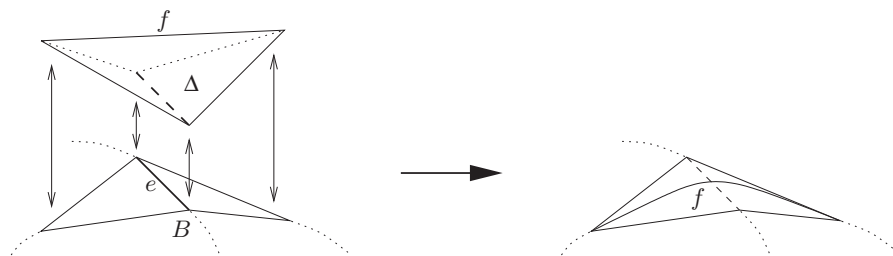


FIGURE 4. Performing a layering.

Definition 2.2. (Layering.) Consider a triangulation with some boundary component B . A *layering* involves attaching a single tetrahedron Δ to the boundary B as follows. Two adjacent faces of Δ are identified directly with two adjacent faces of B , and the remaining two faces of Δ become new boundary faces. This procedure is illustrated in Figure 4.

The underlying 3-manifold is unchanged—the primary effect of the layering is to alter the curves formed by the edges on the boundary. This is illustrated in the right-hand diagram of Figure 4, where the old boundary edge e has been made internal and a new, different, boundary edge f has appeared in its place.

Given Definitions 2.1 and 2.2, we can now define a layered surface bundle precisely.

Definition 2.3. (Layered surface bundle.) A *layered torus bundle* or a *layered Klein-bottle bundle* is a triangulation formed as follows. Let F be either the torus or the Klein bottle. An untwisted I -bundle over F is formed such that each boundary $F \times \{0\}$ and $F \times \{1\}$ consists of precisely two faces. Then zero or more tetrahedra are sequentially layered onto the boundary $F \times \{1\}$, resulting in a new boundary surface F' , again with precisely two faces. Finally, the surfaces $F \times \{0\}$ and F' are identified according to some homeomorphism of the original surface F .

For convenience, we refer to both layered torus bundles and layered Klein-bottle bundles as *layered surface bundles*.

It is clear that the 3-manifold formed from a layered torus bundle or a layered Klein-bottle bundle is a torus bundle or Klein-bottle bundle over the circle. Once again, the reader is referred to Figure 1 for a pictorial representation of this procedure.

2.1.2 Census Triangulations. The layered surface bundles that appear in the census give rise to the follow-

ing 3-manifolds. From layered torus bundles we obtain the six manifolds

$$T^2 \times I / \begin{bmatrix} 1 & 1 \\ 1 & 0 \end{bmatrix}, \quad T^2 \times I / \begin{bmatrix} 0 & 1 \\ 1 & 0 \end{bmatrix}, \quad T^2 \times I / \begin{bmatrix} 1 & 0 \\ 0 & -1 \end{bmatrix}, \\ T^2 \times I / \begin{bmatrix} 2 & 1 \\ 1 & 0 \end{bmatrix}, \quad T^2 \times I / \begin{bmatrix} 3 & 1 \\ 1 & 0 \end{bmatrix}, \quad T^2 \times I / \begin{bmatrix} 3 & 2 \\ 2 & 1 \end{bmatrix}.$$

From layered Klein-bottle bundles we obtain the four flat manifolds

$$T^2 \times I / \begin{bmatrix} 0 & 1 \\ 1 & 0 \end{bmatrix}, \quad T^2 \times I / \begin{bmatrix} 1 & 0 \\ 0 & -1 \end{bmatrix}, \\ \text{SFS}(\mathbb{R}P^2 : (2, 1) (2, 1)), \quad \text{SFS}(\bar{D} : (2, 1) (2, 1)),$$

each of which has an alternative expression as a Klein-bottle bundle over the circle.

Table 3 places these observations within the context of the overall census. Specifically, it lists the number of different layered surface bundles that appear in the census for each number of tetrahedra, as well as the number of distinct 3-manifolds that these layered surface bundles describe. Note that there are only eight distinct 3-manifolds in total, since in the lists above, the torus bundles $T^2 \times I / \begin{bmatrix} 0 & 1 \\ 1 & 0 \end{bmatrix}$ and $T^2 \times I / \begin{bmatrix} 1 & 0 \\ 0 & -1 \end{bmatrix}$ each appear twice.

Again it can be observed that there are significantly more triangulations than 3-manifolds. This is because there are several different choices for the initial thin I -bundle, as well as several different boundary homeomorphisms (and thus several different layerings) that can be used to describe the same 3-manifold.

Tetrahedra	3-Manifolds	Triangulations
6	5 (out of 5)	15 (out of 24)
7	1 (out of 3)	4 (out of 17)
8	2 (out of 10)	12 (out of 59)

TABLE 3. Frequencies of layered surface bundles within the census.

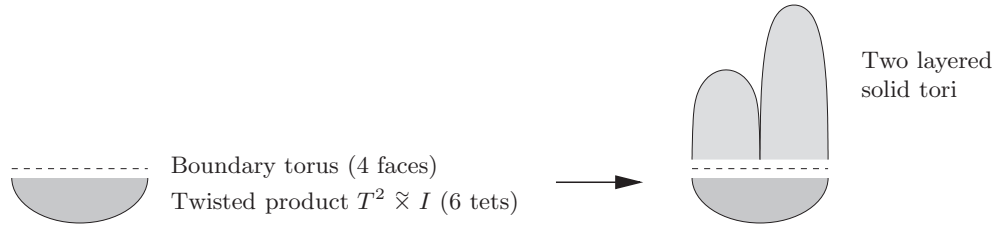


FIGURE 5. Constructing a plugged thin I -bundle.

2.2 Plugged Thin I -Bundles

A *plugged thin I -bundle* is a type of triangulation that allows us to create a nonorientable Seifert fibered space with two exceptional fibers. It begins with a 6-tetrahedron triangulation of the twisted product $T^2 \times I$, which has four boundary faces. Attached to this boundary are two new solid tori. This procedure is illustrated in Figure 5.

The fibration results as follows. Let M^2 represent the Möbius band, and let the orbifold \bar{A} be the annulus with one reflector boundary component and one regular boundary component. The twisted product $T^2 \times I$ can be represented as a trivial Seifert fibered space over either M^2 or \bar{A} (depending on the placement of the fibers).⁴ The two new tori then close off the base orbifold and introduce two exceptional fibers. The resulting 3-manifold is a Seifert fibered space over either $\mathbb{R}P^2$ or \bar{D} with two exceptional fibers.

2.2.1 Components. We now describe details of how the separate components of a plugged thin I -bundle are formed. The original $T^2 \times I$ is triangulated as a *twisted thin I -bundle*, and the two additional tori are triangulated as *layered solid tori*. We describe each of these components in turn.

Definition 2.4. (Twisted thin I -bundle.) A *twisted thin I -bundle* over the torus is a triangulation of the twisted product $T^2 \times I$ formed as follows.

Consider the interval $I = [0, 1]$. The twisted product $T^2 \times I$ is naturally foliated by surfaces $T^2 \times \{x, 1 - x\}$ for $0 \leq x \leq \frac{1}{2}$. For all $x \neq \frac{1}{2}$, this surface is a double cover of the torus $T^2 \times \{\frac{1}{2}\}$.

As in Definition 2.1, we require that this foliation decompose each individual tetrahedron into either triangles or quadrilaterals as illustrated in Figure 2. Once again, we insist that every vertex lie on the boundary $T^2 \times \{0, 1\}$,

as do the upper face in the triangular case and the upper and lower edges in the quadrilateral case.

Again we observe that the surface $T^2 \times \{\frac{1}{2}\}$ meets every tetrahedron in precisely one triangle or quadrilateral. This surface is referred to as the *central torus* of the I -bundle.

An example of a twisted thin I -bundle over the torus is shown in Figure 6. Here we have six tetrahedra arranged into a long triangular prism, whose four back faces form the boundary torus (as shaded in the first diagram). The left and right triangles are identified directly (so that $\triangle ADG$ is identified with $\triangle CFJ$). The upper and lower rectangles are identified with a twist and a translation, so that $\square ABHG$ and $\square HJFE$ are identified and $\square GHED$ and $\square BCJH$ are identified.

The central torus $T^2 \times \{\frac{1}{2}\}$ is shaded in the second diagram of the sequence, and in the third diagram it is made clear how the six tetrahedra divide this torus into four triangles and two quadrilaterals. The arrows on this final diagram indicate how the edges of the central torus are identified.

As with the untwisted thin I -bundles of the previous section, it should be noted that the decomposition of the central torus into triangles and quadrilaterals provides enough information to completely reconstruct the thin I -bundle.

The second component that appears in a plugged thin I -bundle is the *layered solid torus*. Layered solid tori are well understood, and have been discussed by Jaco and Rubinstein [Jaco and Rubinstein 03, Jaco and Rubinstein 06] as well as by Matveev, Martelli, and Petronio in the context of special spines [Matveev 98, Martelli and Petronio 04]. In the context of a census of triangulations they are described and parameterized in [Burton 03]. We omit the details here.

For this overview it suffices to know the following: A layered solid torus is a triangulation of a solid torus containing one vertex, two boundary faces, and three boundary edges, as illustrated in Figure 7. Moreover, it is

⁴More generally, the Seifert fibrations of every I -bundle over the torus or Klein bottle are classified by Amendola and Martelli in [Amendola and Martelli 05 Appendix A].

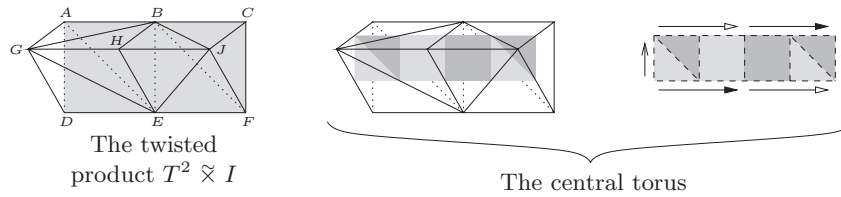


FIGURE 6. An example of a twisted thin I -bundle.

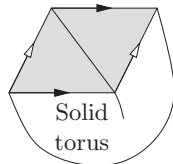


FIGURE 7. The boundary of a layered solid torus.

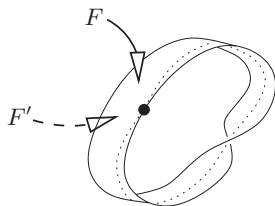


FIGURE 8. A degenerate layered solid torus.

constructed with the explicit aim of making its three boundary edges follow some particular curves along the boundary torus. There are infinitely many different layered solid tori, corresponding to infinitely many different choices of boundary curves.

It is useful to consider the Möbius band as a *degenerate* layered solid torus with zero tetrahedra. That is, the Möbius band formed from a single triangle can be thickened slightly to create a solid torus with two boundary faces F and F' , as illustrated in Figure 8.

We are now ready to define a plugged thin I -bundle.

Definition 2.5. (Plugged thin I -bundle.) A *plugged thin I -bundle* is a triangulation constructed as follows: Begin with a twisted thin I -bundle over the torus. This twisted thin I -bundle must have precisely six tetrahedra and four boundary faces. Furthermore, these boundary faces must form one of the two configurations shown in Figure 9. We refer to these configurations as the *allowable torus boundaries*.



FIGURE 9. The two allowable torus boundaries.

Observe that these boundary faces can be split into two annuli (the left annulus $ABED$ and the right annulus $BCFE$, with edge \overline{BE} distinct from edges \overline{AD} and \overline{CF}). To each of these annuli attach a layered solid torus. These tori must be attached so that edges \overline{AD} , \overline{BE} , and \overline{CF} are identified, and each annulus $ABED$ and $BCFE$ becomes a torus instead. This is illustrated for the first boundary configuration in Figure 10.

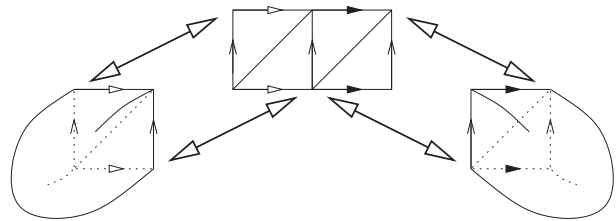


FIGURE 10. Attaching two layered solid tori to the boundary.

Note that either layered solid torus may be degenerate. In this case a one-face Möbius band is inserted, and the two faces of the corresponding boundary annulus are joined to each side of this Möbius band. Since the Möbius band has no thickness, the result is that the two faces of the boundary annulus become joined to each other. An example of this is illustrated in Figure 11, where faces $\triangle CDA$ and $\triangle DAB$ become identified.

Again it may help to refer to Figure 5 for an overview of this construction. The step in which we attach the layered solid tori is a little counterintuitive, since we are essentially using two solid tori to fill just one torus

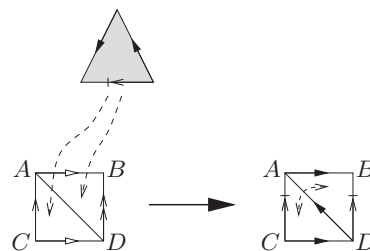


FIGURE 11. Attaching a degenerate layered solid torus to an annulus.

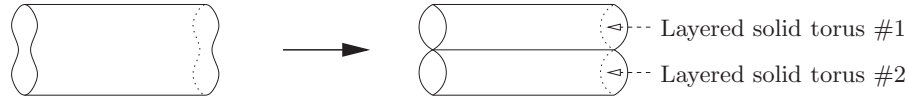


FIGURE 12. Pinching the torus boundary to create two separate tori.

boundary component. Figure 12 illustrates what is really happening—the single torus boundary is pinched along a curve to form two separate torus boundaries, each of which is then filled with a separate layered solid torus.

We can now determine the underlying 3-manifold as follows: The four-face boundary of the twisted $T^2 \tilde{\times} I$ can be filled with vertical fibers, as illustrated in Figure 13. As shown in [Amendola and Martelli 05], this extends to a Seifert fibration of $T^2 \tilde{\times} I$ as a trivial Seifert fibered space over either M^2 or \bar{A} . In the other direction, this extends to a Seifert fibration of each layered solid torus with an exceptional fiber at its center (unless the boundary curves for the layered solid torus are chosen such that the meridional disk of the torus is bounded by a fiber or meets each fiber just once).

The result is a Seifert fibered space over either $\mathbb{R}P^2$ or \bar{D} with two exceptional fibers. See [Burton 03] for a formula that gives the precise Seifert invariants in terms of the individual parameters of the thin I -bundle and the two layered solid tori.



FIGURE 13. Fibers in the two allowable torus boundaries.

2.2.2 Census Triangulations. The plugged thin I -bundles in the census give rise to the Seifert fibered spaces

- SFS ($\mathbb{R}P^2 : (2, 1) (2, 1)$), SFS ($\mathbb{R}P^2 : (2, 1) (3, 1)$),
- SFS ($\mathbb{R}P^2 : (2, 1) (4, 1)$), SFS ($\mathbb{R}P^2 : (2, 1) (5, 2)$),
- SFS ($\mathbb{R}P^2 : (3, 1) (3, 1)$), SFS ($\mathbb{R}P^2 : (3, 1) (3, 2)$),
- SFS ($\bar{D} : (2, 1) (2, 1)$), SFS ($\bar{D} : (2, 1) (3, 1)$),
- SFS ($\bar{D} : (2, 1) (4, 1)$), SFS ($\bar{D} : (2, 1) (5, 2)$),
- SFS ($\bar{D} : (3, 1) (3, 1)$), SFS ($\bar{D} : (3, 1) (3, 2)$).

Table 4 lists the frequencies of plugged thin I -bundles within the overall census. Here the large number of triangulations results from the fact that there are several possible choices for the triangulation of the initial twisted product $T^2 \tilde{\times} I$, as well as the equivalence between some spaces such as SFS ($\mathbb{R}P^2 : (3, 1) (3, 1)$) and SFS ($\mathbb{R}P^2 : (3, 2) (3, 2)$).

Tetrahedra	3-Manifolds	Triangulations
6	2 (out of 5)	4 (out of 24)
7	2 (out of 3)	6 (out of 17)
8	8 (out of 10)	22 (out of 59)

TABLE 4. Frequencies of plugged thin I -bundles within the census.

2.3 Plugged Thick I -Bundles

A *plugged thick I -bundle* is very similar in construction to a plugged thin I -bundle. The difference is that a smaller twisted thin I -bundle is used, but the resulting torus boundary is not one of the allowable torus boundaries of Figure 9. As a result, some additional tetrahedra must be added to reconfigure the torus boundary (thus “thickening” the I -bundle). Once this is done, the two new layered solid tori are attached as before. This procedure is illustrated in Figure 14.

There are two different ways in which this construction can be carried out:

- (i) *We begin with a 3-tetrahedron twisted thin I -bundle over the torus.* An example is shown in Figure 15. The three tetrahedra are arranged into a triangular prism, and the boundary torus is formed from the two back faces (as shaded in the second diagram). The left and right faces are identified directly (with $\triangle ACE$ identified with $\triangle BDF$), and the upper and lower squares are identified with a twist and a translation (with $\triangle EFA$ and $\triangle CDF$ identified and with $\triangle ABF$ and $\triangle EFC$ identified). As usual, the third and fourth diagrams illustrate the central torus $T^2 \times \{\frac{1}{2}\}$.
 The resulting boundary torus has only two faces, which is clearly not an allowable torus boundary (see Definition 2.5 and Figure 9). To compensate, we attach a 3-tetrahedron thickening plug as illustrated in Figure 16. The two back faces of this plug (shaded in the diagram) are attached to the old two-face boundary torus. The four front faces become a new allowable boundary torus, and the upper and lower faces $\triangle ABC$ and $\triangle DEF$ are identified with each other.
- (ii) *We begin with a 5-tetrahedron twisted thin I -bundle over the torus.* This is illustrated in Figure 17, with

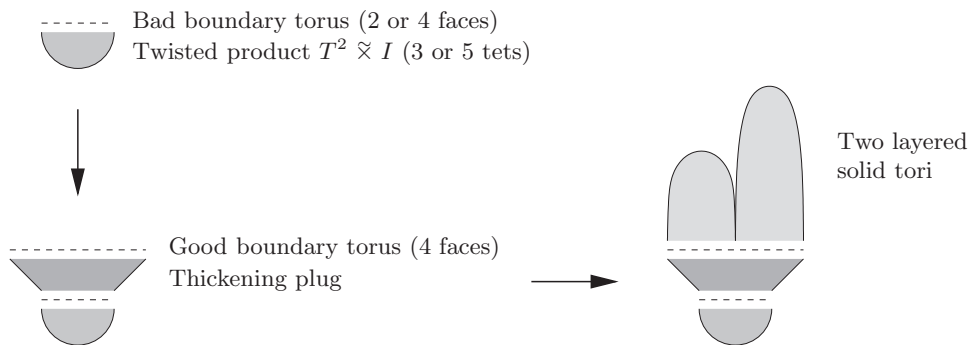


FIGURE 14. Constructing a plugged thick I -bundle.

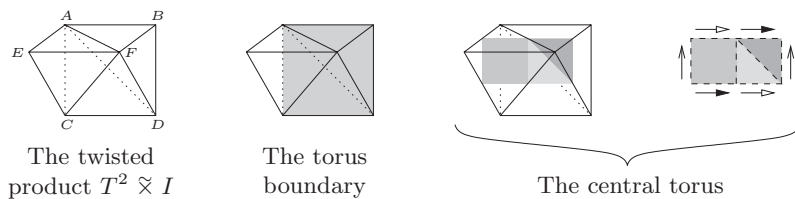


FIGURE 15. A 3-tetrahedron twisted thin I -bundle.

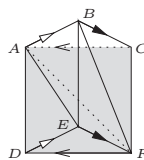


FIGURE 16. A 3-tetrahedron thickening plug.

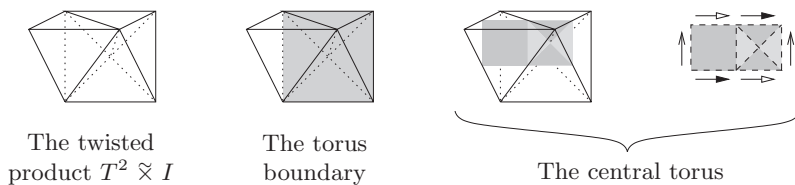


FIGURE 17. A 5-tetrahedron twisted thin I -bundle.

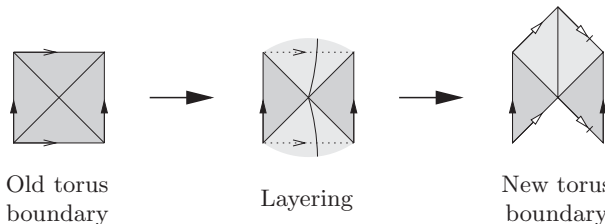


FIGURE 18. Layering to obtain an allowable torus boundary.

the faces of the triangular prism identified as before in Figure 15. Here the torus boundary has four faces, but they are not arranged into an allowable torus boundary. We must therefore reconfigure the boundary edges by performing a layering as il-

lustrated in Figure 18, resulting in a new four-face boundary that satisfies our requirements.

We can formalize this into the following definition. For a complete enumeration of the different I -bundles and

thickening plugs that can be used, the reader is referred to [Burton 03].

Definition 2.6. (Plugged thick I -bundle.) A *plugged thick I -bundle* is a triangulation formed as follows: We begin with a twisted thin I -bundle over the torus, which has either (i) three tetrahedra and two boundary faces, or (ii) five tetrahedra and four boundary faces. We then convert the torus boundary into one of the allowable torus boundaries described in Definition 2.5 (see Figure 9), either by (i) inserting a 3-tetrahedron thickening plug as described above, or (ii) layering a new tetrahedron onto the torus boundary.

We require that the resulting structure be a 6-tetrahedron triangulation of the twisted product $T^2 \tilde{\times} I$ with an allowable torus boundary. We finish the construction by attaching two layered solid tori exactly as described in Definition 2.5.

Since we are producing triangulations of the twisted product $T^2 \tilde{\times} I$ with the same allowable boundary tori used for plugged thin I -bundles, it follows that we should obtain the same underlying 3-manifolds. Specifically, we obtain Seifert fibered spaces over either $\mathbb{R}P^2$ or \bar{D} with two exceptional fibers. Again a precise formula appears in [Burton 03] for calculating the exact Seifert invariants in terms of the individual parameters of the triangulation.

2.3.1 Census Triangulations. The plugged thick I -bundles in the census give rise to the spaces

$$\begin{aligned} \text{SFS}(\mathbb{R}P^2 : (2, 1) (2, 1)), & \quad \text{SFS}(\mathbb{R}P^2 : (2, 1) (3, 1)), \\ \text{SFS}(\mathbb{R}P^2 : (2, 1) (4, 1)), & \quad \text{SFS}(\mathbb{R}P^2 : (2, 1) (5, 2)), \\ \text{SFS}(\mathbb{R}P^2 : (3, 1) (3, 1)), & \quad \text{SFS}(\mathbb{R}P^2 : (3, 1) (3, 2)), \\ \text{SFS}(\bar{D} : (2, 1) (2, 1)), & \quad \text{SFS}(\bar{D} : (2, 1) (3, 1)), \\ \text{SFS}(\bar{D} : (2, 1) (4, 1)), & \quad \text{SFS}(\bar{D} : (2, 1) (5, 2)), \\ \text{SFS}(\bar{D} : (3, 1) (3, 1)), & \quad \text{SFS}(\bar{D} : (3, 1) (3, 2)). \end{aligned}$$

As expected from the similarity in construction, these are exactly the same 12 spaces as the plugged thin I -bundles produce (though none of the specific triangulations are

Tetrahedra	3-Manifolds	Triangulations
6	2 (out of 5)	4 (out of 24)
7	2 (out of 3)	7 (out of 17)
8	8 (out of 10)	25 (out of 59)

TABLE 5. Frequencies of plugged thick I -bundles within the census.

the same). Table 5 lists the frequencies of plugged thick I -bundles within the overall census.

3. OBSERVATIONS AND CONJECTURES

In this section, we pull together observations from the census and form conjectures based on these observations. Following this, we discuss the future of the nonorientable census, including what we might expect to see when the census is extended to higher numbers of tetrahedra.

As explained in the introduction, there is an extremely heavy computational load in creating a census such as this. Each new level of the census (measured by number of tetrahedra, or equivalently by the complexity of Matveev) is an order of magnitude more difficult to construct than the last. At the time of writing, the 9-tetrahedron nonorientable census is under construction, with a healthy body of partial results already obtained.⁵ Each of the conjectures below is consistent with these partial results. We return specifically to the 9-tetrahedron census in Section 3.3.

3.1 Minimal Triangulations

Our first observation relates to the combinatorial structures of nonorientable minimal triangulations. Recall from the introduction that very few sufficient conditions are known for minimal triangulations. Conjectures have been made for various classes of 3-manifolds, but such conjectures are notoriously difficult to prove.

Matveev, Martelli, and Petronio have made a variety of well-grounded conjectures about the smallest number of tetrahedra required for various classes of orientable 3-manifolds [Matveev 98, Martelli and Petronio 04]. Here we form conjectures of this type in the nonorientable case. Moreover, based upon the growing body of experimental evidence, we push further and make conjectures regarding the construction of all minimal triangulations of various classes of nonorientable 3-manifolds.

Section 2 introduces three families of triangulations: (i) layered surface bundles, (ii) plugged thin I -bundles, and (iii) plugged thick I -bundles. It is easy enough to see that these families produce (i) torus or Klein-bottle bundles over the circle and (ii, iii) Seifert fibered spaces over $\mathbb{R}P^2$ or \bar{D} with two exceptional fibers. What is less obvious is that *every* minimal triangulation of such a 3-manifold should belong to one of the three families listed above.

⁵The 9-tetrahedron and 10-tetrahedron censuses were completed in 2006 and are described in [Burton 06]. These newer results remain consistent with the conjectures presented in this paper.

In fact, the evidence supports this suggestion, with the exception of the four flat manifolds at the lowest (6-tetrahedron) level of the census. Although most 3-manifolds have many different minimal triangulations (up to 10 in some cases), these minimal triangulations all belong to the three families above. The partial results for the 9-tetrahedron census also support this hypothesis, even though a much wider variety of triangulations is found at this level (as discussed below in Section 3.3). We are therefore led to make the following conjectures.

Conjecture 3.1. *Let M be a torus bundle over the circle that is not one of the flat manifolds*

$$T^2 \times I / \begin{bmatrix} 0 & 1 \\ 1 & 0 \end{bmatrix}, \quad T^2 \times I / \begin{bmatrix} 1 & 0 \\ 0 & -1 \end{bmatrix}.$$

Then every minimal triangulation of M is a layered torus bundle, as described by Definition 2.3.

Moreover, at least one minimal triangulation of M has at its core the 6-tetrahedron product $T^2 \times I$ illustrated in Figure 3. In other words, this 6-tetrahedron product $T^2 \times I$ may be used as a starting point for constructing a minimal triangulation of M .

Conjecture 3.2. *Let M be a Seifert fibered space over either $\mathbb{R}P^2$ or \bar{D} with precisely two exceptional fibers. Moreover, suppose that M is not one of the flat manifolds SFS ($\mathbb{R}P^2 : (2, 1) (2, 1)$), SFS ($\bar{D} : (2, 1) (2, 1)$). Then every minimal triangulation of M is either a plugged thin I -bundle or a plugged thick I -bundle, as described by Definitions 2.5 and 2.6.*

Note that if these conjectures are true, the number of tetrahedra in such a minimal triangulation is straightforward to calculate. The number of layerings required to obtain a particular set of boundary curves is well described by Martelli and Petronio [Martelli and Petronio 04], though in the equivalent language of special spines. Similar calculations in the language of triangulations and layered solid tori have been described by Jaco and Rubinstein in a variety of informal contexts.

What remains then is to calculate the number of tetrahedra that are not involved in layerings. For Conjecture 3.1 we can assume this to be the 6-tetrahedron product $T^2 \times I$ of Figure 3, and for Conjecture 3.2 we can simply count the six additional tetrahedra involved in the twisted product $T^2 \tilde{\times} I$ to which our layered solid tori are attached.

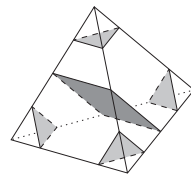


FIGURE 19. Normal disks within a tetrahedron.

3.2 Central Surfaces

Our next observation is regarding embedded surfaces within nonorientable 3-manifolds. Recall that all three families of triangulations described in Section 2 begin with a thin I -bundle. The central surface of this thin I -bundle is an embedded surface meeting each tetrahedron of the thin I -bundle in either a single quadrilateral or a single triangle.

This is reminiscent of the theory of normal surfaces. Normal surfaces, first introduced by Kneser [Kneser 29] and subsequently developed by Haken [Haken 61, Haken 62], play a powerful role in algorithms in 3-manifold topology. A *normal surface* within a triangulation meets each tetrahedron in one or more *normal disks*, which are either triangles separating one vertex from the other three or quadrilaterals separating two vertices from the other two. A variety of normal disks can be seen in Figure 19.

It follows then that the central surface of a thin I -bundle is a special type of normal surface, namely one that meets each tetrahedron of the thin I -bundle in one and only one normal disk. This leads us to make the following more general definition.

Definition 3.3. (Central Normal Surface.) Let N be an embedded normal surface in a 3-manifold triangulation. We refer to N as a *central normal surface* if N meets each tetrahedron of the triangulation in at most one normal disk (i.e., one triangle, one quadrilateral, or nothing).

Note that we have replaced “one and only one” with “at most one,” since the central surface of a thin I -bundle does not meet the tetrahedra involved in the other parts of the triangulation (such as the layered solid tori in a plugged thin I -bundle).

It can be observed that every triangulation in this census contains a central normal surface. This is to be expected, since a thin I -bundle appears at the core of every family described in Section 2. This observation is more general, however, as shown by the following result.

Theorem 3.4. *Every triangulation of a closed nonorientable 3-manifold contains a central normal surface.*

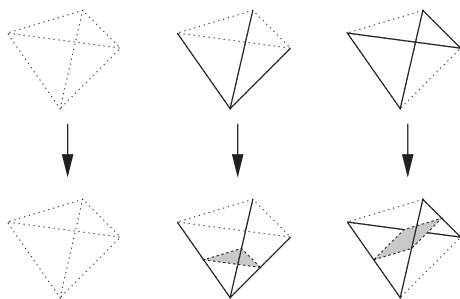


FIGURE 20. Constructing a central surface from black and white edges.

An outline of a proof is sketched below; thanks are due to Matveev and Rubinstein for independently suggesting the approach.

Proof: The edges of such a triangulation can be colored black or white as follows. Let τ be a maximal tree in the 1-skeleton of the triangulation, and color each edge of τ white. Each remaining edge represents a path from τ back to itself; color such an edge white if this path is orientation-preserving within the 3-manifold, or black if it is orientation-reversing. Note that since the manifold is nonorientable, there is at least one black edge.

It is straightforward to see that the black edges of each tetrahedron must form one of the patterns illustrated in the upper half of Figure 20 (where solid lines represent black edges and dotted lines represent white edges). We can insert normal disks into the tetrahedra as illustrated in the lower half of the figure, so that each black edge meets exactly one disk, and each white edge meets none. These disks can be seen to fit together to form a central normal surface as required. \square

Central normal surfaces have proven invaluable for analyzing census triangulations by hand. They are quickly enumerated, and once a well-positioned central surface has been found, the surrounding structures often become simpler to analyze and understand.

Moreover, Theorem 3.4 may well offer a starting point for the proofs of Conjectures 3.1 and 3.2—as with the central surface of a thin I -bundle, a central normal surface can be used to reconstruct the portion of the triangulation that surrounds it, which may then lead to new structural results.

It is worth noting that Theorem 3.4 does not hold in the orientable case. Of the 191 closed orientable minimal irreducible triangulations with six or fewer tetrahedra,⁶ only 118 have a central normal surface.

⁶These triangulations are enumerated in [Matveev 98] in the equivalent language of special spines.

3.3 Future Directions

As mentioned in the introduction, the triangulations and 3-manifolds seen in the 8-tetrahedron census offer little variety beyond what has already been seen in the censuses of seven and fewer tetrahedra. The primary advantage of the 8-tetrahedron census has been the larger body of data (an additional 59 triangulations and 10 distinct 3-manifolds) that has supported the formulation of the conjectures above.

Clearly, a greater variety must appear in the census at some point, since there are far more nonorientable 3-manifolds than those described by the families of Section 2. The question is how much larger the census must become before we begin to see them.

Fortunately, the answer is, not much larger at all. As discussed at the beginning of Section 3, the 9-tetrahedron census is currently under construction, and a significant body of partial results is already available. In addition to the 3-manifolds already described (torus bundles over the circle and Seifert fibered spaces over $\mathbb{R}P^2$ or \bar{D} with two exceptional fibers), the 9-tetrahedron results include the following:

- *Seifert fibered spaces over $\mathbb{R}P^2$ and \bar{D} with three exceptional fibers.* In particular, the spaces

$$\text{SFS}(\mathbb{R}P^2 : (2, 1) (2, 1) (2, 1))$$

and

$$\text{SFS}(\bar{D} : (2, 1) (2, 1) (2, 1))$$

are found.

- *Seifert fibered spaces over several other base orbifolds with one exceptional fiber.* The base orbifolds include the torus, the Klein bottle, the annulus with two reflector boundaries, and the Möbius strip with one reflector boundary. In each case a single $(2, 1)$ exceptional fiber is found.
- *Manifolds with nontrivial JSJ composition.* In particular, a number of spaces are found that begin with a Seifert fibered space over the annulus with a single $(2, 1)$ fiber, followed by a nontrivial identification of the two torus boundaries.

It is therefore hoped that once completed, the 9-tetrahedron census can offer richer insights into the structures of nonorientable minimal triangulations than what we have seen to date.

Moving beyond the 9-tetrahedron census, one might ask how much further we must go before we move

Δ	3-Manifold	Triangulations
6	$T^2 \times I / \begin{bmatrix} 1 & 1 \\ 1 & 0 \end{bmatrix}$	$B_{T_6^2 -1,1 1,0}$
	$T^2 \times I / \begin{bmatrix} 0 & 1 \\ 1 & 0 \end{bmatrix}$	$B_{T_6^1 -1,0 -1,1}, B_{T_6^1 0,-1 -1,0}, B_{T_6^1 0,1 1,0} = B_{K_6^2 0,-1 -1,0},$ $B_{T_6^1 1,0 1,-1}, B_{K_6^1 0,-1 -1,0}, E_{6,3}$
	$T^2 \times I / \begin{bmatrix} 1 & 0 \\ 0 & -1 \end{bmatrix}$	$B_{T_6^2 1,0 0,-1}, B_{K_6^1 1,0 0,1}, B_{K_6^2 1,0 0,1}$
	SFS ($\mathbb{R}P^2 : (2, 1) (2, 1)$)	$B_{K_6^1 0,1 1,0}, B_{K_6^2 0,1 1,0}, H_{\tilde{T}_6^1}, H_{\tilde{T}_6^2}, H_{\tilde{T}_6^3},$ $K_{\tilde{T}_5^1}, K_{\tilde{T}_5^2}, K_{\tilde{T}_5^3}, E_{6,2}$
	SFS ($\bar{D} : (2, 1) (2, 1)$)	$B_{K_6^1 -1,0 0,-1}, B_{K_6^2 -1,0 0,-1}, H_{\tilde{T}_6^4}, K_{\tilde{T}_5^4}, E_{6,1}$
7	$T^2 \times I / \begin{bmatrix} 2 & 1 \\ 1 & 0 \end{bmatrix}$	$B_{T_6^2 -1,1 2,-1}, B_{T_6^2 0,-1 -1,2}, B_{T_7 -1,-1 -1,0}, B_{T_7 1,1 1,0}$
	SFS ($\mathbb{R}P^2 : (2, 1) (3, 1)$)	$H_{\tilde{T}_6^1 3,-2}, H_{\tilde{T}_6^1 3,-1}, H_{\tilde{T}_6^2 3,-2}, H_{\tilde{T}_6^2 3,-1}, H_{\tilde{T}_6^3 3,-1},$ $K_{\tilde{T}_5^1 3,-1}, K_{\tilde{T}_5^2 3,-2}, K_{\tilde{T}_5^2 3,-1}, K_{\tilde{T}_5^3 3,-2}, K_{\tilde{T}_5^3 3,-1}$
	SFS ($\bar{D} : (2, 1) (3, 1)$)	$H_{\tilde{T}_6^4 3,-1}, K_{\tilde{T}_5^4 3,-2}, K_{\tilde{T}_5^4 3,-1}$
8	$T^2 \times I / \begin{bmatrix} 3 & 1 \\ 1 & 0 \end{bmatrix}$	$B_{T_6^2 -3,1 1,0}, B_{T_6^2 -2,3 1,-1}, B_{T_6^2 -1,3 1,-2},$ $B_{T_7 -2,-1 -1,0}, B_{T_7 -1,-1 -2,-1}, B_{T_7 2,1 1,0},$ $B_{T_8^1 -1,-1 -1,0}, B_{T_8^1 1,1 1,0}, B_{T_8^2 0,1 1,1}, B_{T_8^2 1,1 1,0}$
	$T^2 \times I / \begin{bmatrix} 3 & 2 \\ 2 & 1 \end{bmatrix}$	$B_{T_6^2 -1,2 2,-3}, B_{T_7 -1,-2 -1,-1}$
	SFS ($\mathbb{R}P^2 : (2, 1) (4, 1)$)	$H_{\tilde{T}_6^1 4,-3}, H_{\tilde{T}_6^1 4,-1}, H_{\tilde{T}_6^2 4,-3}, H_{\tilde{T}_6^2 4,-1}, H_{\tilde{T}_6^3 4,-1},$ $K_{\tilde{T}_5^1 4,-1}, K_{\tilde{T}_5^2 4,-3}, K_{\tilde{T}_5^2 4,-1}, K_{\tilde{T}_5^3 4,-3}, K_{\tilde{T}_5^3 4,-1}$
	SFS ($\mathbb{R}P^2 : (2, 1) (5, 2)$)	$H_{\tilde{T}_6^1 5,-3}, H_{\tilde{T}_6^1 5,-2}, H_{\tilde{T}_6^2 5,-3}, H_{\tilde{T}_6^2 5,-2}, H_{\tilde{T}_6^3 5,-2},$ $K_{\tilde{T}_5^1 5,-2}, K_{\tilde{T}_5^2 5,-3}, K_{\tilde{T}_5^2 5,-2}, K_{\tilde{T}_5^3 5,-3}, K_{\tilde{T}_5^3 5,-2}$
	SFS ($\mathbb{R}P^2 : (3, 1) (3, 1)$)	$H_{\tilde{T}_6^1 3,-1 3,-2}, H_{\tilde{T}_6^2 3,-1 3,-2}, H_{\tilde{T}_6^3 3,-1 3,-2},$ $K_{\tilde{T}_5^1 3,-1 3,-2}, K_{\tilde{T}_5^2 3,-2 3,-1}, K_{\tilde{T}_5^2 3,-1 3,-2}, K_{\tilde{T}_5^3 3,-1 3,-2}$
	SFS ($\mathbb{R}P^2 : (3, 1) (3, 2)$)	$H_{\tilde{T}_6^1 3,-2 3,-2}, H_{\tilde{T}_6^1 3,-1 3,-1}, H_{\tilde{T}_6^2 3,-2 3,-2},$ $H_{\tilde{T}_6^2 3,-1 3,-1}, H_{\tilde{T}_6^3 3,-1 3,-1}, K_{\tilde{T}_5^1 3,-1 3,-1},$ $K_{\tilde{T}_5^2 3,-1 3,-1}, K_{\tilde{T}_5^3 3,-2 3,-2}, K_{\tilde{T}_5^3 3,-1 3,-1}$
	SFS ($\bar{D} : (2, 1) (4, 1)$)	$H_{\tilde{T}_6^4 4,-1}, K_{\tilde{T}_5^4 4,-3}, K_{\tilde{T}_5^4 4,-1}$
	SFS ($\bar{D} : (2, 1) (5, 2)$)	$H_{\tilde{T}_6^4 5,-2}, K_{\tilde{T}_5^4 5,-3}, K_{\tilde{T}_5^4 5,-2}$
	SFS ($\bar{D} : (3, 1) (3, 1)$)	$H_{\tilde{T}_6^4 3,-1 3,-1}, K_{\tilde{T}_5^4 3,-2 3,-1}, K_{\tilde{T}_5^4 3,-1 3,-2}$
	SFS ($\bar{D} : (3, 1) (3, 2)$)	$H_{\tilde{T}_6^4 3,-1 3,-2}, K_{\tilde{T}_5^4 3,-1 3,-1}$

TABLE 6. All 18 distinct 3-manifolds and their 100 minimal triangulations.

away from graph manifolds. It was proven by Matveev [Matveev 90] that the first hyperbolic manifolds to appear in the orientable census are those of smallest known volume (first seen at nine tetrahedra). It is reasonable to expect the same of the nonorientable census; the candidate smallest-volume nonorientable hyperbolic manifold described by Hodgson and Weeks [Hodgson and Weeks 94] can be triangulated with 11 tetrahedra, though neither the minimality of the volume nor the minimality of the triangulation has been proven.

Finally it must be noted that any extension of the census will require new improvements in the algorithm—the worse-than-exponential growth of the search space means that increased computing power is not enough. Ideally, such improvements would involve a blend of topological results (such as those seen in [Burton 04a]) and pure algorithmic optimizations. The expected yield from higher levels of the census is a great incentive, and so work on the enumeration algorithm is continuing.

4. APPENDIX: TRIANGULATIONS FROM THE CENSUS

For convenience we include a list of all 100 triangulations from the census, named according to the precise parameterizations described in [Burton 03]. See Table 6. This allows the reader to cross-reference triangulations and constructions between these two papers. In summary, we have the following:

- Triangulations $H_{\tilde{T}...}$ are plugged thin I -bundles, and triangulations $K_{\tilde{T}...}$ are plugged thick I -bundles.
- Triangulations $B_{T...}$ are layered torus bundles, and triangulations $B_{K...}$ are layered Klein-bottle bundles. Note that there is one triangulation of $T^2 \times I / \begin{bmatrix} 0 & 1 \\ 1 & 0 \end{bmatrix}$ that can be expressed in both forms.
- Triangulations $E_{6,1}$, $E_{6,2}$, and $E_{6,3}$ are described in [Burton 03] as exceptional triangulations. However, both $E_{6,1}$ and $E_{6,2}$ are also layered Klein-bottle bundles whose central Klein bottles were not originally included in the parameterization of [Burton 03].
- More specifically, triangulations $B_{T_n...}$ and $B_{K_n...}$ are constructed from thin I -bundles containing precisely n tetrahedra. The four triangulations named $B_{T_8...}$ are not included in the parameterization of [Burton 03], since 8-tetrahedron thin I -bundles were not covered.

For full details, including a precise explanation of the parameterization system, the reader is referred to [Burton 03].

ACKNOWLEDGMENTS

Special thanks must go to J. Hyam Rubinstein for many helpful discussions throughout the course of this research, as well as to the anonymous referees for their thoughtful suggestions. Thanks are also due to the University of Melbourne and the Victorian Partnership for Advanced Computing, both of which have provided computational support for this and related research.

REFERENCES

- [Amendola and Martelli 03] Gennaro Amendola and Bruno Martelli. “Non-orientable 3-Manifolds of Small Complexity.” *Topology Appl.* 133:2 (2003), 157–178.
- [Amendola and Martelli 05] Gennaro Amendola and Bruno Martelli. “Non-orientable 3-Manifolds of Complexity up to 7.” *Topology Appl.* 150:1-3 (2005), 179–195.
- [Burton 03] Benjamin A. Burton. “Structures of Small Closed Non-orientable 3-Manifold Triangulations.” To appear in *J. Knot Theory Ramifications*, 2003.
- [Burton 04a] Benjamin A. Burton. “Face Pairing Graphs and 3-Manifold Enumeration.” *J. Knot Theory Ramifications* 13:8 (2004) 1057–1101.
- [Burton 04b] Benjamin A. Burton. “Introducing Regina, the 3-Manifold Topology Software.” *Experiment. Math.* 13:3 (2004), 267–272.
- [Burton 05] Benjamin A. Burton. “Regina: Normal Surface and 3-Manifold Topology Software.” Available online (<http://regina.sourceforge.net/>), 1999–2005.
- [Burton 06] Benjamin A. Burton. “Enumeration of Non-Orientable 3-Manifolds Using Face Pairing Graphs and Union-Find.” To appear in *Discrete Comput. Geom.*, 2006.
- [Callahan et al. 99] Patrick J. Callahan, Martin V. Heidebrand, and Jeffrey R. Weeks. “A Census of Cusped Hyperbolic 3-Manifolds.” *Math. Comp.* 68:225 (1999), 321–332.
- [Casali 98] Maria Rita Casali. “Classification of Nonorientable 3-Manifolds Admitting Decompositions into ≤ 26 Coloured Tetrahedra.” *Acta Appl. Math.* 54:1 (1998), 75–97.
- [Casali 04] Maria Rita Casali. “Computing Matveev’s Complexity of Non-orientable 3-Manifolds via Crystallization Theory.” *Topology Appl.* 144 (2004), 201–209.
- [Frigerio et al. 03] Roberto Frigerio, Bruno Martelli, and Carlo Petronio. “Complexity and Heegaard Genus of an Infinite Class of Compact 3-Manifolds.” *Pacific J. Math.* 210:2 (2003), 283–297.
- [Haken 61] Wolfgang Haken. “Theorie der Normalflächen.” *Acta Math.* 105 (1961) 245–375.

- [Haken 62] Wolfgang Haken. “Über das Homöomorphieproblem der 3-Mannigfaltigkeiten. I.” *Math. Z.* 80 (1962), 89–120.
- [Hodgson and Weeks 94] Craig D. Hodgson and Jeffrey R. Weeks. “Symmetries, Isometries and Length Spectra of Closed Hyperbolic Three-Manifolds.” *Experiment. Math.* 3:4 (1994), 261–274.
- [Jaco and Rubinstein 03] William Jaco and J. Hyam Rubinstein. “0-Efficient Triangulations of 3-Manifolds.” *J. Differential Geom.* 65:1 (2003), 61–168.
- [Jaco and Rubinstein 06] William Jaco and J. Hyam Rubinstein. “Layered-Triangulations of 3-Manifolds.” Preprint, 2006.
- [Kneser 29] Hellmuth Kneser. “Geschlossene Flächen in dreidimensionalen Mannigfaltigkeiten.” *Jahresbericht der Deut. Math.-Verein.* 38 (1929), 248–260.
- [Martelli 06] Bruno Martelli. “Complexity of 3-Manifolds.” In *Spaces of Kleinian Groups*, pp. 91–120, London Math. Soc. Lecture Note Ser. 329. Cambridge: Cambridge Univ. Press, 2006.
- [Martelli and Petronio 01] Bruno Martelli and Carlo Petronio. “Three-Manifolds Having Complexity at Most 9.” *Experiment. Math.* 10:2 (2001), 207–236.
- [Martelli and Petronio 02] Bruno Martelli and Carlo Petronio. “A New Decomposition Theorem for 3-Manifolds.” *Illinois J. Math.* 46 (2002), 755–780.
- [Martelli and Petronio 04] Bruno Martelli and Carlo Petronio. “Complexity of Geometric Three-Manifolds.” *Geom. Dedicata* 108:1 (2004), 15–69.
- [Matveev 90] Sergei V. Matveev. “Complexity Theory of Three-Dimensional Manifolds.” *Acta Appl. Math.* 19:2 (1990), 101–130.
- [Matveev 98] Sergei V. Matveev. “Tables of 3-Manifolds up to Complexity 6.” Max-Planck-Institut für Mathematik Preprint Series 67, 1998. Available online (http://www.mpim-bonn.mpg.de/html/pre_-prints/preprints.html).
- [Matveev 05] Sergei V. Matveev. “Recognition and Tabulation of Three-Dimensional Manifolds.” *Dokl. Akad. Nauk* 400:1 (2005), 26–28.

Benjamin A. Burton, Department of Mathematics, SMGS, RMIT University, GPO Box 2476V, Melbourne, VIC 3001, Australia (bab@debian.org)

Received September 5, 2005; accepted in revised form March 9, 2006.